FATIGUE CONSIDERATIONS FOR THE DESIGN OF RAILROAD BRIDGES

Manfred A. Hirt, Swiss Federal Institute of Technology,
Lausanne, Switzerland

This paper describes a concept for the fatigue evaluation and design of railroad bridges. The primary objective is to account for the number of stress cycles per train, the corresponding stress ranges, and the total number of trains in the lifetime of the structure. Stress recordings from various structural elements of existing bridges were used as input for fatigue tests on beams. The test results are evaluated using the rainflow counting method and Miner's cumulative damage law. These results show good correspondence with constant amplitude test data. The assessment of traffic is based on theoretical traffic models and on measurements of axle loads and axle spacings. The fatigue effect of the traffic models is simulated by computer programs in terms of span length and compared to field measurements. It is shown that a correction factor may be applied to the design live load when used for fatigue considerations. In addition, the fatigue design concept enables to account for the total number of trains in the lifetime of the bridge. Also, a different safety factor may be applied for redundant and non-redundant load path structures.

Introduction

The collapse of a given structure due to fatigue depends on the fatigue behaviour of its different structural elements. The governing stresses causing fatigue damage in these elements are due to actual traffic conditions. For railroad bridges, the actual traffic may be described by axle loads and axle spacings for every train, and by the total number of train crossings during the lifetime of the bridge (Figure 1).

However, one has to bear in mind that it is impossible for a design engineer to consider actual traffic conditions except for the average number of trains per day. It is therefore important to adjust the design live load in such a way that the corrected live load may account for the actual traffic.

It is obvious that a brittle material may considerably shorten the lifetime of a structure. Hence, fatigue and brittle fracture are not independent (1, 2). It is therefore important that a sudden failure without preceding large deformations should be excluded either by using a sufficiently ductile material (3), or by adopting a highly redundant structural system. For the following discussion it is assumed that brittle fracture is not the governing mode of collapse.

Figure 1. Passenger train and a typical short span steel bridge.

Constant Amplitude Fatigue Strength

An extremely large amount of experimental test data on steel beams has been obtained since 1967 from a study sponsored by the National Cooperative Highway Research Program and carried out at the Fritz Engineering Laboratory of Lehigh University. These studies have shown that the most important factors which govern the fatigue strength are the stress range and the type of details, regardless of the type of steel (4, 5). Comprehensive specifications based on the stress range concept have been developed in the USA and are actually proposed in different countries in Europe.

Figure 2 shows the design categories proposed for the Swiss specifications for steel structures (6). An additional category A1 has been added for bolted connections, and the 95 % survival limits have been adjusted to a slope of m = 3 in the double-

Figure 2. Allowable fatigue stress ranges according to Swiss specifications for steel construction.

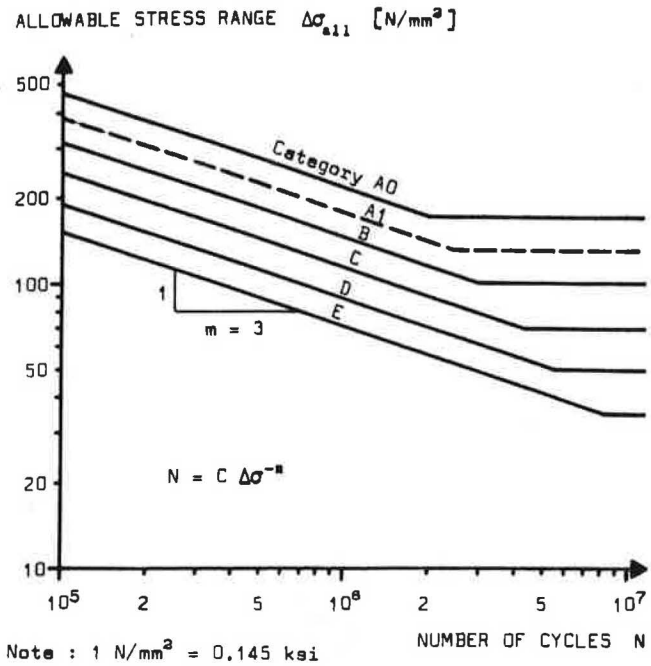

logarithmic representation.

$$N = C\ \Delta\sigma^{-m} \qquad (1)$$

It will be shown that the parallel lines enable to consider the cumulative damage due to traffic stresses independently of design categories. This may not be true when the fatigue limit becomes important since the cut-off points are not always located at the same number of cycles.

The proposed fatigue strength categories had to be confirmed for typical design details and fabrication procedures used in Switzerland and Europe. The test results (7, 8) show good correspondence with previous results and the proposed categories appear to give a conservative estimate for all details tested.

Variable Amplitude Fatigue Strength

Figure 3 shows actual live load stresses in three different structural elements of the riveted bridges shown in Figure 1. Each bridge is built up of two riveted plate girders of 19.5 m (64 ft) span length and of floorbeams every 2.44 m (8 ft). The stringers, located under the rails and connected to the webs of the floorbeams support the wooden ties.

Figure 3. Typical live load stresses in three different structural elements and for two types of trains.

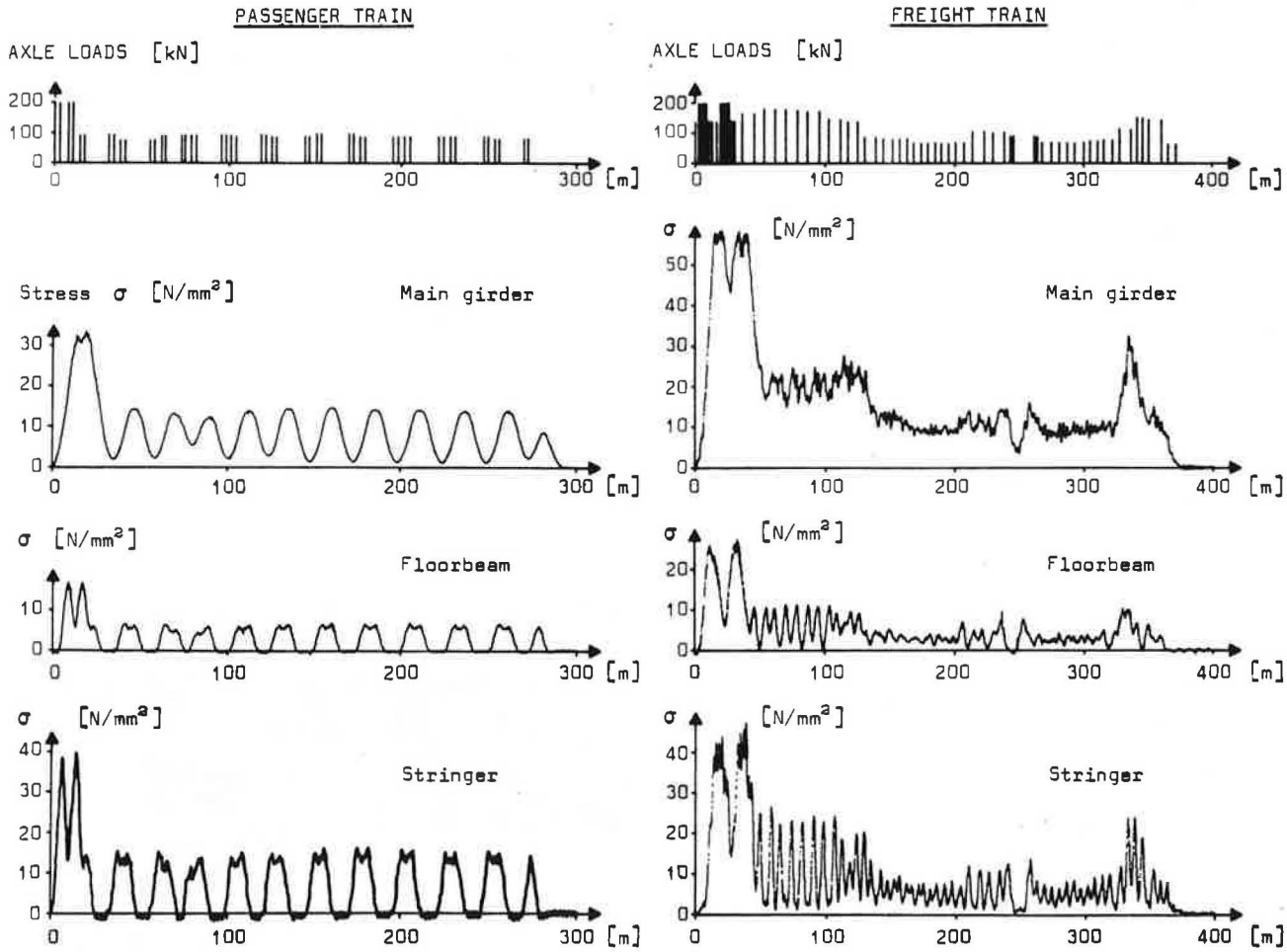

Note : 1 kN = 0.225 kip , 1 N/mm² = 0.145 ksi , 1 m = 3.28 ft

The recordings show quite regular stress fluctuations under the passage of the passenger train, they are much more random under the freight train. The locomotives of both train types cause predominant stress peaks.

The question arises as to how to treat (statistically and theoretically) such recordings in order to assess the cumulative fatigue damage of the stress fluctuations.

Figure 4. Comparaison of three different categories of stress-time diagrams.

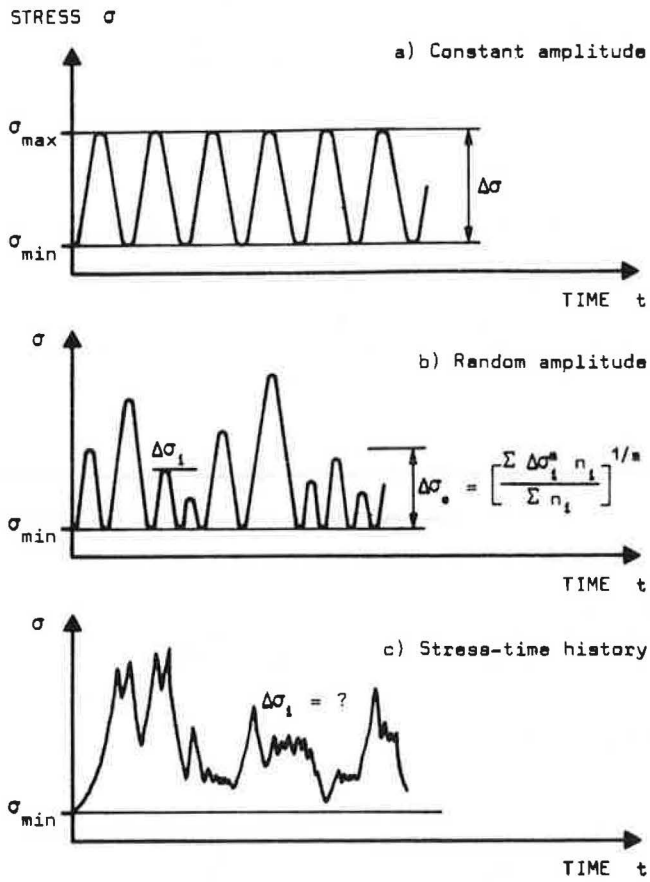

Figure 5. Schematic representation of the rainflow counting method.

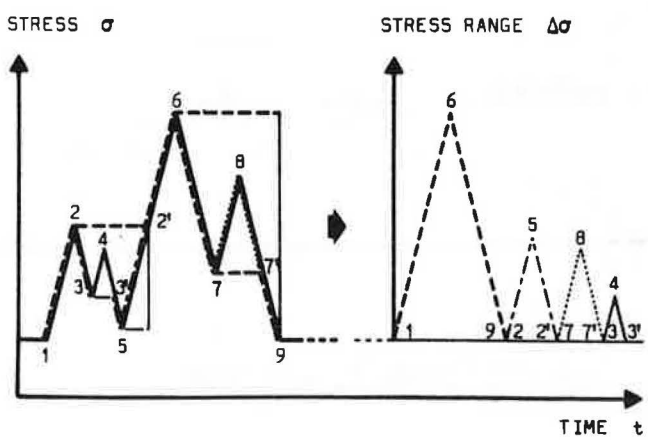

Equivalent Stress Range

General stress-time histories (Figure 4 c) have to be correlated to constant amplitude data (Figure 4 a). This may be done in two steps :

1. The first step consists in defining and counting the individual stress ranges $\Delta\sigma_i$ of a given stress-time history. This procedure assumes a priori the validity of the stress range concept. Hence, of the many counting methods available (9) only those can be used that adequatly define stress ranges. The European railroad convention (UIC : Union Internationale de Chemins de fer) has proposed to apply the rainflow counting method (10) of which a graphical representation is shown in Figure 5. It can be shown that the results of the rainflow count correspond well to those given by the range pair count. However, the rainflow method presents the advantage that the cut-off level for small stress cycles does not have to be fixed in advance.

2. The second step relates the fatigue effect of the above defined stress ranges $\Delta\sigma_i$ to an equivalent constant amplitude stress range $\Delta\sigma_e$ (11). Based on the cumulative damage law of Palmgren-Miner and the fatigue strength lines according to equation 1, the equivalent stress range $\Delta\sigma_e$ becomes

$$\Delta\sigma_e = \left[\frac{\Sigma\ \Delta\sigma_i^m\ n_i}{\Sigma\ n_i}\right]^{1/m} \qquad (2)$$

where m is the slope of the lines without consideration of the fatigue limits.

This second step had been shown to be a conservative approach to account for the cumulative damage of random stress cycles (12). However, it is important to note that the assumptions for the first and second steps are not necessarily independent. Only test results can confirm the validity of the hypotheses.

Stress History Fatigue Tests

Stress recordings from passages of different types of trains were used for fatigue tests at the Swiss Federal Institute of Technology. The test set-up of Figure 6 shows two 500 kN (110 tons) hydraulic jacks, two load cells, and a test beam as well as the electronic control panels. This closed loop system with a capacity of 250 litres of oil per minute (65 gpm) was designed and fabricated by F + W Emmen, Switzerland.

Figure 6. Fatigue test simulator.

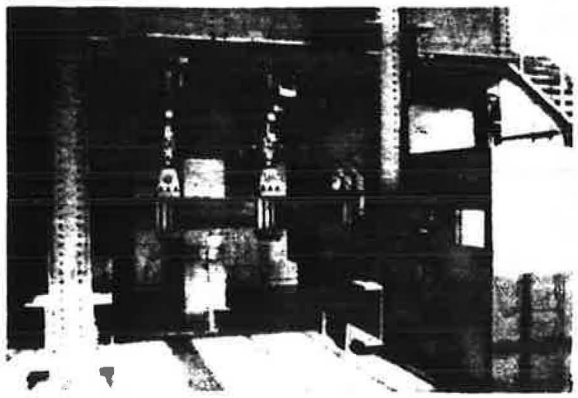

One set of test results of cover-plated beams is shown in Figure 7. The number of stress cycles corresponds to the total number of cycles counted, and the equivalent stress range is calculated using equation 2 with m = 3. Also included are five results from constant amplitude tests. It can be seen that the tests using stress-time histories give results comparable to constant amplitude data.

However, it should be noted that a slightly better correlation between test results might be obtained using an exponent m greater than 3. Additional tests on beams with gusset plates welded to the tension flange (13) yield similar results. More tests are under way to further investigate the correlation between actual stress histories and constant amplitude test data.

Considering the many influencing parameters of actual traffic, it shall be assumed that equation 2 is sufficiently accurate. The next question is therefore, how to obtain the number of stress cycles and the corresponding equivalent stress ranges for every structural element.

Figure 7. Fatigue test results of cover-plated beams subjected to real stress-time histories.

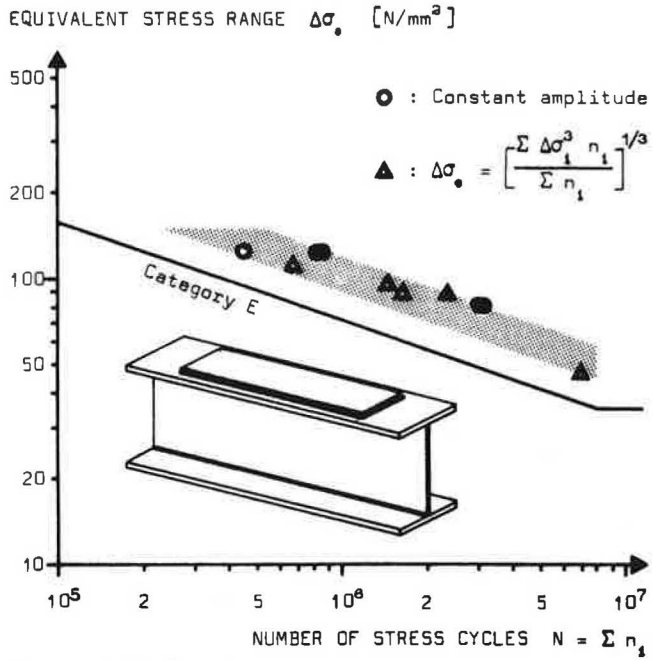

Note : 1 N/mm² = 0.145 ksi

Effect of Traffic Loads

Traffic Models

One of the traffic models used for computer simulation is shown in Figure 8. It is representative of the rolling stock and assumes a certain number of passenger trains, differently loaded freight trains, and some block trains. Up to a total number of 150 trains per day in each direction have already been recorded on a double track line in Switzerland.

The above defined traffic is used to compute the number of stress cycles and the equivalent stress ranges. This can be done for different shapes of influence lines, such as for a simple span bridge,

Figure 8. Traffic model (Swiss Federal Railroads) used for a computer analysis of the effect of actual traffic on railroad bridges.

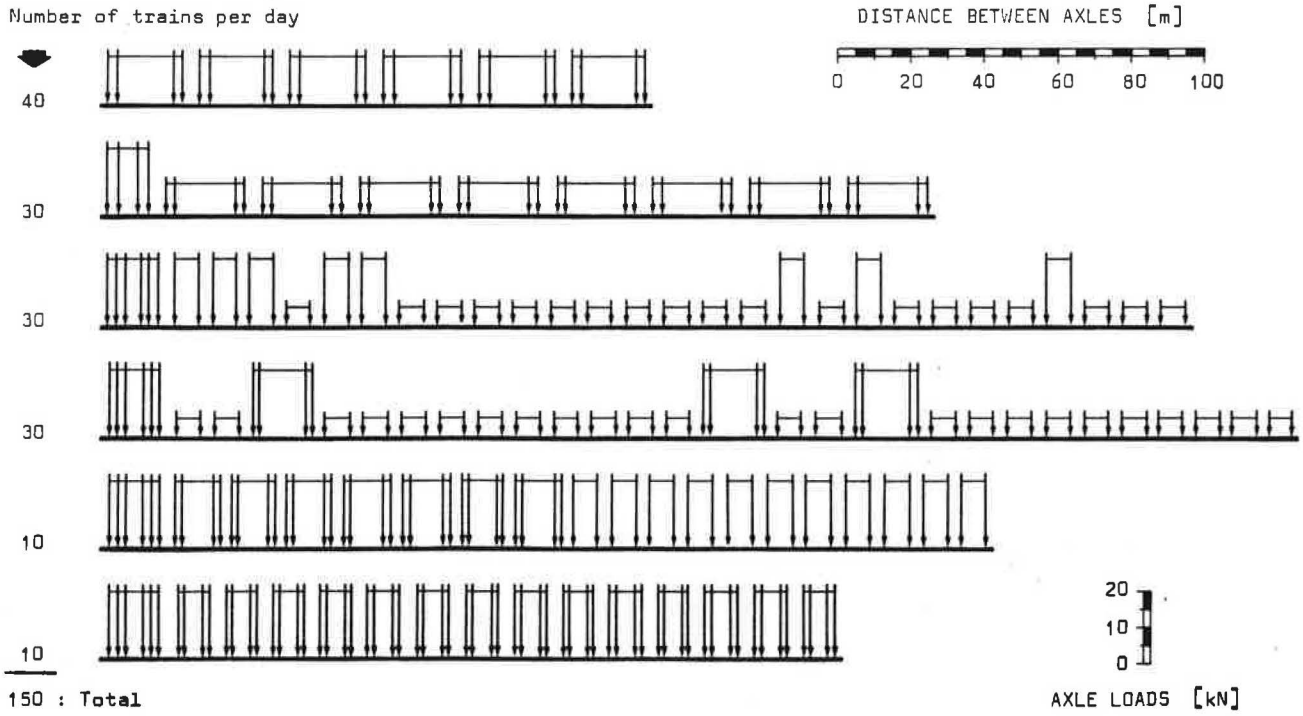

Note : 1 kN = 0.225 kip , 1 m = 3.28 ft

continuous bridge or a stringer on spring supports. However, in order to avoid computing stresses, the effect of the traffic is directly compared to the effect of the UIC design live load, shown in Figure 9.

The equivalent stress range $\Delta\sigma_e$ and the maximum stress range $\Delta\sigma_{max}$ of the traffic model are compared in Figure 10 to the stress range due to the UIC live load. The corresponding number of stress cycles in terms of span length are shown in Figure 11. The following observations can be made from these two figures :

1. The maximum stress range remains generally below 70 % of the UIC design stress range. This value shall be used later on when the effect of the fatigue limits are discussed.
2. The equivalent stress range $\Delta\sigma_e$ amounts to approximately 40 % of the UIC design stress range, depending only slightly on span length.
3. The corresponding number of stress cycles, given as an average number of cycles per train greatly depends on span length. For very short spans, almost every axle causes a major stress cycle, then for spans up to 20 m (65 ft) approximately one cycle per car occurs, and for longer spans only one cycle per train is observed. It should be noted that all stress ranges smaller than 10 % of the UIC design stress range have been neglected.

The two parameters, equivalent stress range $\Delta\sigma_e$ and average number of cycles per train N_{av}, can now be used to assess the fatigue life of a given structure. Also, their fatigue damage can be compared to the theoretical damage due to the UIC design stress range.

Correction Factor

The fatigue life, expressed in number of trains N_t for a given structural element is

$$N_t = \frac{C\ \Delta\sigma_e^{-m}}{N_{av}} \qquad (3)$$

when $\Delta\sigma$ in equation 1 is replaced by the equivalent stress range $\Delta\sigma_e$ for the traffic model, and the corresponding number of stress cycles per train N_{av} is accounted for. Conversely, the design stress range $\Delta\sigma_{uic}$ can be adjusted by a correction factor $\varkappa$ in such a way that the same number of theoretical load applications results :

$$N = N_t = C\ (\varkappa\ \Delta\sigma_{uic})^{-m} \qquad (4)$$

The comparison of the right hand sides of equations 3 and 4 yield the correction factor

$$\varkappa = \frac{\Delta\sigma_e}{\Delta\sigma_{uic}}\ N_{av}^{\ 1/m} \qquad (5)$$

Both terms of equation 5 ($\Delta\sigma_e/\Delta\sigma_{uic}$ and N_{av}) have already been given in Figures 10 and 11. Hence, the correction factor can be computed. This can be done regardless of design categories provided the slope m of the fatigue strength lines (Figure 2) is the same.

The heavy line in Figure 12 shows the resulting correction factor for the traffic model used. A strong influence of span length is apparent ; the values increase rapidly with decreasing span length (14). This obviously reflects the greater number of

Figure 9. UIC design live load (UIC : Union Internationale des Chemins de fer).

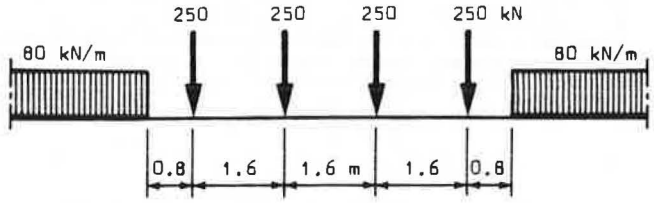

Note : 1 kN = 0.225 kip , 1 kN/m = 68.6 pounds per foot

Figure 10. Comparison of the maximum and equivalent stress ranges due to the traffic model with the stress range due to the UIC design load.

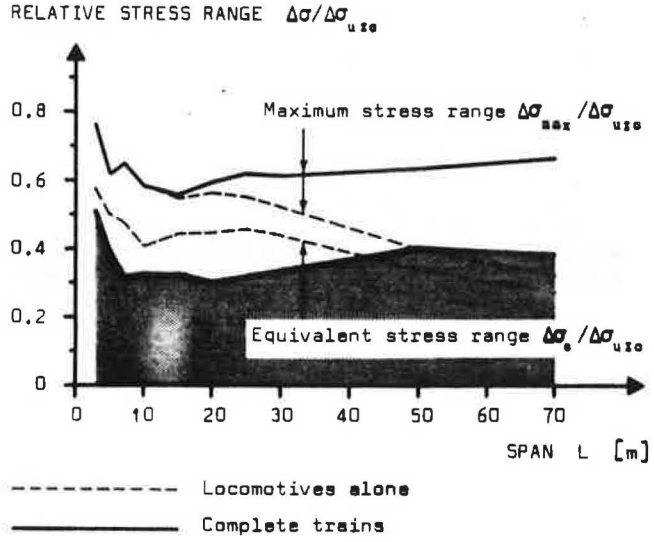

Figure 11. Average number of major stress cycles per train depending on span length.

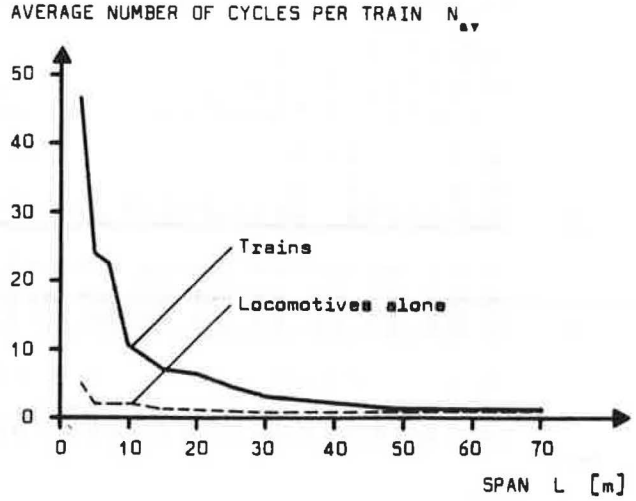

stress cycles per train for shorter spans. Similar curves have been obtained for different European countries representing various traffic models.

Comparison with Actual Traffic

Equation 5 gives a correction factor based on a traffic model and on theoretical influence lines. It is of interest to compare these values with values derived from stress recordings ; a few results (14, 15) are shown in Figure 12. It can be seen that the measured values for the main girder correspond well to the theoretical value, but the values for the floorbeam and stringer are substantially below the calculated values. This might be explained as follows :

Figure 12. Correction factor applied to the UIC design load in order to account for the cumulative fatigue damage of actual service traffic.

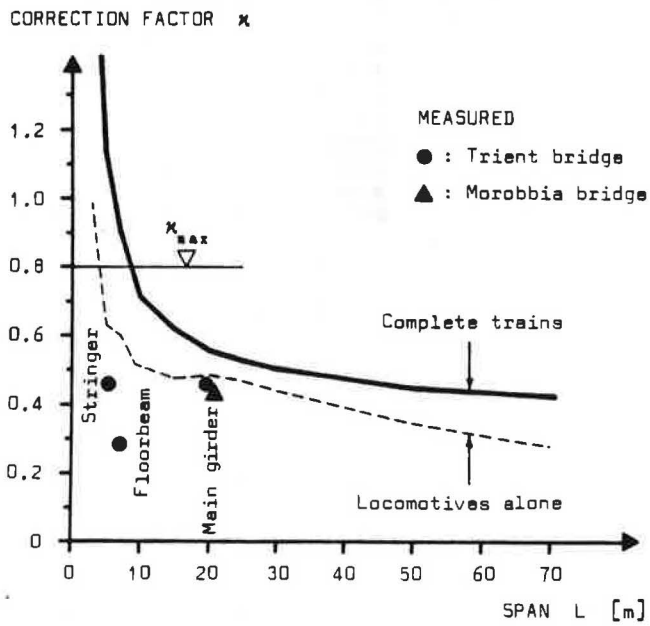

1. The actual axle loads measured were generally smaller than those used for the traffic model, in particular a smaller percentage of heavy freight trains and trains with two locomotives were observed.
2. The design stress range $\Delta\sigma_{u\,zc}$ includes an impact factor to account for dynamic effects. This impact factor is quite important for short spans, typically about 50 % for a span of 5 metres (15 ft). However, stress recordings showed much smaller impact values.
3. The statical behaviour of bridges is generally more favorable than assumed in structural analysis due to load distribution effects and greater redundacy of the structural elements.
4. The design of short elements, like floorbeams and stringers, is often based on stiffness because of deflection limitations. Hence, actual traffic stresses are quite small.

The comparison between measured and theoretical reduction factors (which is not affected by the actual number of trains) indicates a certain margin of safety. However, the few experimental results available to date do not enable to attribute numerical values to this margin of safety. Studies are under way in different European countries to obtain more data.

Fatigue Design Concept

Based on the preceding results and conclusions, the following fatigue design rule is proposed :

$$\kappa\ \Delta\sigma_{u\,zc} \leq \frac{1}{\gamma}\ \Delta\sigma_{all}\ (N_t\ ;\ \text{Category}) \qquad (6)$$

1. The left hand side (load side) considers the design stress range $\Delta\sigma_{u\,zc}$ based on the static design live load, including impact, but adjusted by a correction factor κ (Figure 12) such as to account for the cumulative fatigue damage of actual traffic.
2. The right hand side (strength side) defines the allowable fatigue strength $\Delta\sigma_{all}$ in terms of the total number of trains N_t in the lifetime of the structure, and according to the design category of a given detail (Figure 2).
3. The safety factor can be adjusted to differentiate between redundant and non-redundant load path structures.

The design engineer simply uses the regular design live load to compute the design stress range at a given point in the structure. This value is then corrected to account for the cumulative fatigue damage of actual traffic, where the correction factor is defined in terms of span length for a simple span element, or in terms of the influence length for redundant elements. The fatigue strength for the given structural detail is obtained in terms of the predicted number of trains in the lifetime of the structure.

The same concept may be applied to evaluate the remaining fatigue life of existing bridges. A different correction factor may be used respectively for past, present and future traffic.

Influence of the Fatigue Limit

It is obvious that for a great daily traffic, for example 150 trains, and design lifetime of the structure, for example 100 years, the total number of trains becomes very large ; for the values cited about 5.5 million. For most design categories, this number is greater than the number of cycles N_f of the fatigue limit. Hence, equation 6 could be replaced by

$$\kappa\ \Delta\sigma_{u\,zc} \leq \frac{1}{\gamma}\ \Delta\sigma_f\ (\text{Category}) \qquad (7)$$

This is still too conservative, in particular for small spans, since the reduction factor is obtained without consideration of the fatigue limit. In fact, one must only assure that every stress range $\Delta\sigma_i$, in particular the largest stress range $\Delta\sigma_{max}$, remains below the fatigue limit σ_f ; or analytically

$$\Delta\sigma_{max} \leq \frac{1}{\gamma}\ \Delta\sigma_f \qquad (8)$$

Comparing the left hand sides of equations 7 and 8, a limit for κ can be defined,

$$\varkappa_{max} = \frac{\Delta\sigma_{max}}{\Delta\sigma_{uic}} \qquad (9)$$

which amounts to approximately 0.7 according to the values shown in Figure 10.

Small Number of Trains

The general equation 6 is valid, but the limiting value $\varkappa_{max}$ has to be adjusted :

$$\varkappa_{max} = \frac{\Delta\sigma_{max}}{\Delta\sigma_{uic}} \left[\frac{N_f}{N_t}\right]^{1/m} \qquad (10)$$

N_f is again the number of cycles at the cut-off point for the fatigue limit, and $N_t \leq N_f$ corresponds to the total number of trains in the lifetime of the structure. It is seen that the numerical values of $\varkappa_{max}$ depend on the design category since the fatigue limits do not intersect the fatigue strength lines at the same number of cycles N_f (Figure 2).

Conclusion

The primary objective of this paper is to account for the fatigue effects of actual traffic on railroad bridges. Based on the stress range concept for the fatigue strength, the fatigue damage of stress-time histories are related to constant amplitude test data using the rainflow counting method and Miner's cumulative damage law. The design stress range is then related to the effects of actual traffic or traffic models by a correction factor. As a result, it is shown that design engineers may use the usual design live load and adjust the resulting stress range by this correction factor. The only additional information needed for design is the number of trains in the lifetime of the structure. This number, based on actual or predicted traffic volumes, has to be fixed by the railroad administration.

Acknowledgments

Much of the research discussed in this paper was carried out at the Federal Institute of Technology, Lausanne, Switzerland, under the sponsorship of the Swiss Federal Railroad Administration, the Swiss Federal Department of Transport and the Swiss National Science Foundation. Appreciation is also expressed to the staff at the Institute for Steel Construction.

References

1. Scheffey, C.F. Point Pleasant Bridge Collapse - Conclusion of the Federal Study. ASCE Civil Engineering, 7, 1971, pp. 41-45.
2. Madison, R.B. and Irwin, G.R. Fracture Analysis of King's Bridge, Melbourne. ASCE Journal of the Structural Division, ST9, 1971, pp. 2229-2244.
3. Roberts, R. and Irwin, G.R. Fatigue and Fracture of Bridge Steels. ASCE Journal of the Structural Division, ST2, 1976, pp. 337-353.
4. Fisher, J.W., Frank, K.H., Hirt, M.A. and McNamee, B.M. Effect of Weldments on the Fatigue Strength of Steel Beams. NCHRP Report 102, Highway Research Board, Washington D.C., 1970.
5. Fisher, J.W. et al. : Fatigue Strength of Steel Beams with Transverse Stiffeners and Attachments. NCHRP Report 147, Highway Research Board, Washington D.C., 1974.
6. Schweizerischer Ingenieur- und Architekten-Verein. Steel Structures, SIA Norm 161-E, Zürich, 1978.
7. Hirt, M.A. and Crisinel, M. La résistance à la fatigue des poutres en âme pleine composées-soudées, - Effet des plaquettes et goussets soudés à l'aile. Ecole Polytechnique Fédérale de Lausanne, ICOM 017, 1975.
8. Hirt, M.A. and Crisinel, M. La résistance à la fatigue des poutres en âme pleine composées-soudées, - Effet des détails constructifs et comparaison avec la norme. Ecole Polytechnique Fédérale de Lausanne, ICOM (en préparation).
9. Buxbaum, O. Statistische Zählverfahren als Bindeglied zwischen Beanspruchungsmessung und Betriebsfestigkeitsversuch. Laboratorium für Betriebsfestigkeit, TB-65, Darmstadt, 1966.
10. International Union of Railways. Statistical Distribution of Axle Loads and Stresses in Railway Bridges - Introduction and Definitions. ORE Report D 128/RP1, Utrecht, 1973.
11. Swanson, S.R. Random Load Fatigue : State of the Art Survey. Materials Research and Standards, April, 1968, pp. 10-44.
12. Schilling, C.G., Klippstein, K.H., Barsom, J.M. and Blake, G.T. Fatigue of Welded Steel Bridge Members under Variable-Amplitude Loadings. Final Report NCHRP Project 12-12, Transportation Research Board, Washington D.C., 1975.
13. Hirt, M.A. and Jacquemoud, J. Analyse des essais préliminaires sous charges aléatoires par la méthode de la différence de contraintes équivalente. Ecole Polytechnique Fédérale de Lausanne, ICOM (en préparation).
14. Wolchuk, R. and Mayrbaurl, R.M. Stress Cycles for Fatigue Design of Railroad Bridges. ASCE Journal of the Structural Division, ST1, 1976, pp. 203-213.
15. Jaccard, A. Comportement à la fatigue des ponts-rails. Travail de diplôme, Ecole Polytechnique Fédérale de Lausanne, ICOM, 1976.
16. Hirt, M.A. and Hausammann, H. Betriebsfestigkeit von Eisenbahnbrücken in Verbundbauweise am Beispiel der Morobbia-Brücke. Ecole Polytechnique Fédérale de Lausanne, ICOM 027, 1976.